Memoir of the Fukui Prefectural Dinosaur Museum 17: 9–26 (2018)

ARTICLE

WHEN DID THE DEPOSITION OF THE TETORI GROUP TERMINATE?

Mitsuhiro NAGATA[1], Yoshimi HAYASHI[2], Tomokazu SAKASHITA[2], Yuta KAWAGOE[1], Yoshikazu KOUCHI[1], Satoshi HIRASAWA[3], Masato FUJITA[3], Koshi YAMAMOTO[4], and Shigeru OTOH[1]

[1] Graduate School of Science and Engineering, University of Toyama, 3190 Gofuku, Toyama 930-8555, Japan
[2] Department of Earth Sciences, Faculty of Science, University of Toyama, 3190 Gofuku, Toyama 930-8555, Japan
[3] Toyama Science Museum, 1-8-31 Nishinakano-machi, Toyama 939-8084, Japan
[4] Graduate School of Environmental Studies, Nagoya University, Furo-cho, Chikusa-ku, Nagoya 464-8601, Japan

ABSTRACT

We examined the zircon U-Pb age of the following samples to constrain (1) the minimum age of sedimentation of the Tetori Group (*sensu stricto*) and (2) the period of deposition of the Tetori Group (*s.s.*) in the Jinzu Region: a tuff sample of the Hayashidani Andesite in the Hakusan Region, three samples of felsic dikes cutting the Tetori Group (*s.s.*) in the Hakusan and Jinzu Regions, and a tuff sample from the Tetori Group (*s.s.*) in the Jinzu Region. As a result, the ages of the Hayashidani Andesite and felsic dikes fell between 109 Ma and 104 Ma (middle Albian). The tuff from the Tetori Group (*s.s.*) in the Jinzu Region yielded the concordia age of 120.9 ± 1.1 Ma (2σ; early Aptian), which we interpret as the age of sedimentation. Our geochronologic study, together with previous studies, suggests that the period of sedimentation of the Tetori Group (*s.s.*) included the early Aptian and terminated by the middle Albian. Moreover, recently reported Albian zircon fission-track ages from the Tetori Group (*s.s.*) are likely rejuvenation ages caused by the heat from the igneous activity that formed the felsic dikes.

Key words : Cretaceous, Jinzu Group, Tetori Group, U-Pb age, zircon

長田充弘・林　芳美・坂下智和・川越雄太・高地吉一・平澤　聡・藤田将人・山本鋼志・大藤　茂（2018）手取層群の堆積はいつ終了したか．福井県立恐竜博物館紀要 17：9–26.

狭義の手取層群の堆積年代下限値を求め，神通区の狭義の手取層群の堆積期間を拘束するため，以下の試料のジルコンU-Pb年代を測定した：白山区の林谷安山岩の凝灰岩，白山・神通両区で狭義の手取層群を切る珪長質岩脈３試料，および神通区の狭義の手取層群中の凝灰岩である．林谷安山岩の凝灰岩および珪長質岩脈３試料の年代は，104–109 Ma（白亜紀Albian期中葉）であった．また，神通区の手取層群中の凝灰岩から，堆積年代と解釈される 120.9 ± 1.1 Ma（Aptian期前半）のコンコーディア年代が得られた．本研究と先行研究から，狭義の手取層群の堆積期間はAptian期前半を含み，Albian期中葉には終了していたと考えられる．今回，神通区から得られた珪長質岩脈の年代は，近年先行研究で得られたAlbian期に相当するジルコンフィッション・トラック（FT）年代値に近い．このFT年代は，岩脈をもたらした火成活動による若返り年代と見られる．

INTRODUCTION

The Tetori Group (*sensu lato*; *sensu* Sano, 2015) is distributed in Fukui, Ishikawa, Gifu, Toyama, and Niigata Prefectures, central Japan and consists mostly of Middle Jurassic to Early Cretaceous marine to terrestrial clastic rocks (e.g., Maeda, 1961; Sakai et al., 2012; Sano, 2015; Yamada, 2017; Fig. 1). It overlies unconformably or tectonically Early Jurassic and older rocks of the Hida and Hida Gaien Belts, and middle Cretaceous andesitic to rhyolitic volcanic and pyroclastic rocks, in turn, cover the Tetori Group (*s.l.*). Maeda (1961) divided the distribution area of the Tetori Group (*s.l.*) into the Hakusan and Jinzu Regions; the former includes the Tedorigawa, Kuzuryugawa, Shokawa, and Furukawa–Kamitakara areas surrounding Mt. Hakusan, whereas the latter ranges from the Jinzu basin (the area drained by the Jinzugawa River) to the Northern Japan Alps.

Received July 29, 2018. Accepted November 16, 2018.
Corresponding author — Mitsuhiro NAGATA
E-mail: d1671202＊ems.u-toyama.ac.jp

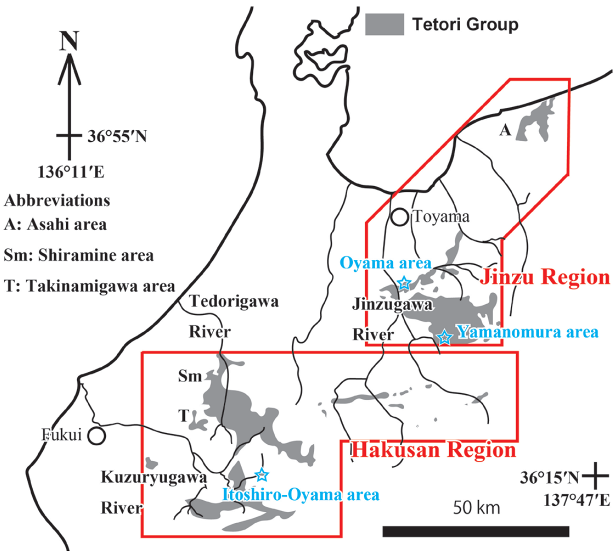

FIGURE 1. Index map showing the distribution of the Tetori Group (*sensu lato*) and the extent of the Hakusan and Jinzu Regions. Modified after Maeda (1961) and Sano (2015). Blue stars denote study areas.

The Tetori Group (*s.l.*) in the Hakusan Region was traditionally subdivided into the Kuzuryu, Itoshiro, and Akaiwa Subgroups in ascending order (Maeda, 1961). On the other hand, several opinions of the lithostratigraphic subdivision have been proposed for the Tetori Group (*s.l.*) in the Jinzu Region. For example, Kawai and Nozawa (1958) subdivided the group into the Higashisakamori, Nagatogawa, and Atotsugawa Formations, in ascending order, and correlated them with the Kuzuryu, Itoshiro, and Akaiwa Subgroups, respectively. Maeda (1961) expressed a different opinion that there is no apparent difference between the Itoshiro and Akaiwa Subgroups in the Jinzu Region and lumped them as the undivided Itoshiro-Akaiwa Subgroup. The depositional age of marine beds in the Kuzuryu and Itoshiro Subgroups has been relatively well constrained using index fossils such as ammonoids. For example, the Kaizara and Yambarazaka Formations of the Kuzuryu Subgroup in the Itoshiro area, Fukui Prefecture, have been correlated with the upper Bathonian–Callovian and Oxfordian, respectively (Sato and Westermann, 1991). Further, the Itsuki Formation of the Itoshiro Subgroup has been correlated with the Hauterivian (–Barremian), because it yields common brackish fauna with the Hauterivian (–Barremian) Ryoseki Formation of the Monobegawa Group in central Shikoku, the Outer Zone of Southwest Japan (Kozai et al., 2002). The depositional age of non-marine beds in the Itoshiro and Akaiwa Subgroups, on the other hand, was hard to constrain, because of the following reasons. (1) The non-marine beds yield no index fossils; (2) there are significant lateral facies changes; and (3) there are no key beds that are useful to correlate the Tetori Group (*s.l.*) in different areas or regions.

Some recent studies proposed the revision of the stratigraphic subdivision of the Tetori Group (*s.l.*) of Maeda (1961). For example, Matsukawa et al. (2014a, b) intended to subdivide the Tetori Group (*s.l.*) in the Jinzu Region into the Tetori (former Kuzuryu Subgroup) and Jinzu (former Itoshiro and Akaiwa Subgroups) Groups. Matsukawa et al. (2014a, b) suggested that the Jinzu Group differs in lithostratigraphy from the Itoshiro and Akaiwa Subgroups in the Hakusan Region; the Itoshiro Subgroup in the Hakusan Region contains marine to brackish deposits whereas the Jinzu Group does not. Matsukawa et al. (2014a) also suggested that the Jinzu Group is younger than the Itoshiro and Akaiwa Subgroups in the Hakusan Region that yield no Aptian–Albian or younger fossils; they obtained Aptian–Albian zircon fission track (FT) ages from four tuffaceous sandstone samples from the lower part of the Jinzu Group. However, the FT age of the three samples among the four from the Yamanomura area, Gifu Prefecture, is inconsistent with the stratigraphy; i.e., Aptian beds overlies an Albian bed. Gifu-ken Dinosaur Fossil Excavation Party (1997) mapped many dikes and sills in the Yamanomura area. Sano (2015) and Yamada (2017), on the other hand, proposed to separate the marine Kuzuryu Subgroup from the Tetori Group (*s.l.*), because (1) the sedimentary environments of the Kuzuryu Subgroup (mostly marine) and the Itoshiro and Akaiwa Subgroups (primarily non-marine) are significantly different and (2) the Kuzuryu Subgroup is some five million years older than the upper subgroups. Sano (2015) and Yamada (2017) subdivided the Tetori Group (*s.l.*) into the Kuzuryu (former Kuzuryu Subgroup) and Tetori Groups (*sensu stricto*; former Itoshiro and Akaiwa Subgroups). Sano (2015) further recognized four depositional stages (DS) in the Middle Jurassic to early Late Cretaceous strata in the Hakusan Region. DS1 is the stage of deposition of mainly marine strata, represented by the Middle–Late Jurassic Kuzuryu Group. DS2–3 is the stage of deposition of mainly brackish to fluvial strata, represented by the Berriasian–Aptian Tetori Group (*s.s.*). DS4 is the stage of deposition of volcanic rocks covering the Tetori Group (*s.s.*), together with the intrusion of some plutonic bodies. We will follow the terminology of Sano (2015) and Yamada (2017) for the Tetori Group (*s.l.*) in the Hakusan Region and will follow the terminology of Kawai and Nozawa (1958) for the Tetori Group (*s.l.*) in the Jinzu Region.

In this study, we present some new zircon U-Pb age data from (1) an andesitic tuff of DS4 that covers the Tetori Group (*s.s.*) in the Itoshiro-Oyama area of the Hakusan Region, (2) felsic intrusive rocks of DS4 that cut the Tetori Group in the Yamanomura area of the Jinzu Region, and (3) a tuff layer of the Tetori Group (*s.s.*) in the Oyama area of the Jinzu Region. The age of andesitic tuff and felsic dikes of DS4 will constrain the minimum age of sedimentation of the Tetori Group. The age of the tuff layer in the Jinzu Region will constrain the age of deposition of the Tetori Group (*s.s.*) there.

Further, we will discuss the temporal relation between the Tetori Group and the Kanmon Group in the Renge, Akiyoshi, Maizuru and Ultra-Tamba Belts, to the south of the Hida and Hida Gaien Belts, Inner Zone of Southwest Japan. The Kanmon Group and the uppermost part of the Tetori Group commonly contain red beds, indicative of the similar sedimentary environment (Maeda, 1961). The Kanmon Group also contains abundant andesitic to rhyolitic volcanic and pyroclastic rocks.

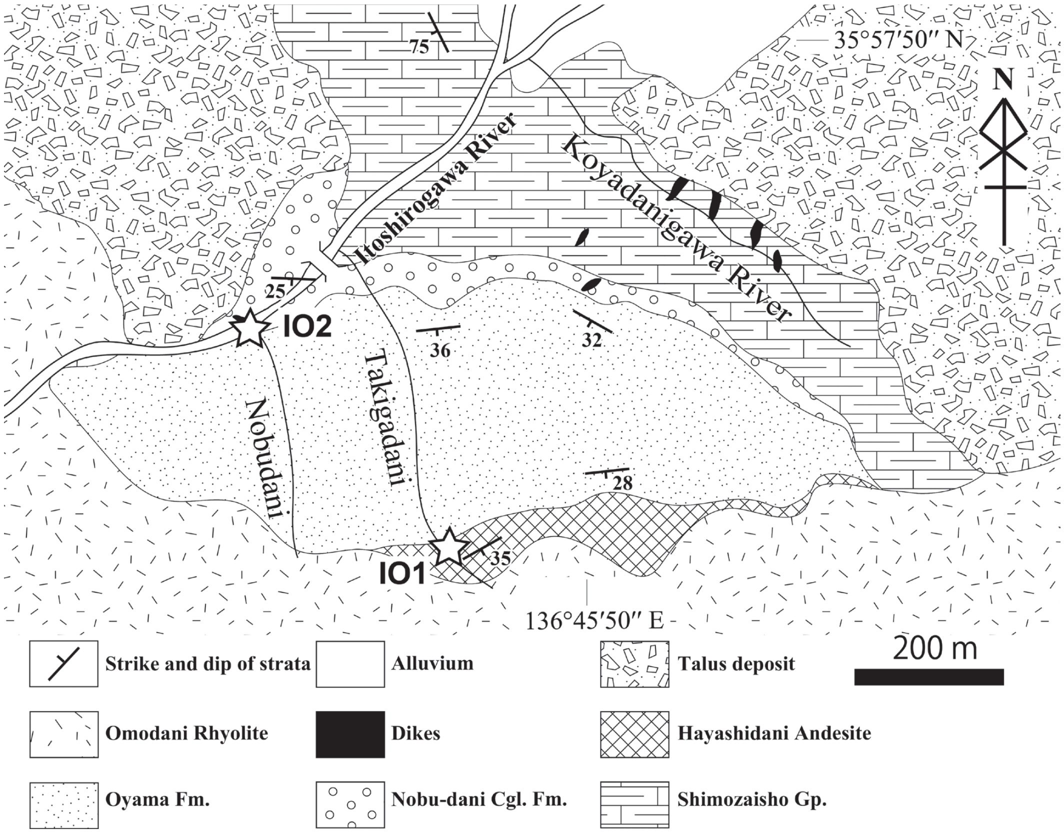

FIGURE 2. Geologic map of the Itoshiro-Oyama area in the Hakusan Region. Modified after Maeda (1957). Stars denote sampling locations of this study. Abbreviations—Cgl.: Conglomerate, Fm: Formation, Gp.: Group.

GEOLOGIC SETTING

Itoshiro-Oyama area in the Hakusan Region (Fig. 2)

The Itoshiro-Oyama area is along the Itoshirogawa River in Gujo City, Gifu Prefecture. The Tetori Group in this area unconformably covers Paleozoic beds (Shimozaisho Group) composed mostly of limestone and mudstone (Kawai, 1959) and consists of the Nobu-dani (Conglomerate) and Oyama Formations in ascending order. The two comformable formations strike east and dip 20°–40°S. The Nobu-dani Formation consists mostly of conglomerate with minor amounts of yellow brown to white sandstone. The sandstone and the matrix of the conglomerate have partly become reddish. The conglomerate contains subangular to round pebbles of limestone and mudstone (Maeda, 1957). The Oyama Formation consists of conglomerate and partly reddish or greenish sandstone and mudstone. The conglomerate mainly contains pebbles of granite, gneiss, and sandstone. Limestone- and mudstone-pebbles are rare. Although Maeda (1957) subdivided the Oyama Formation into the sandstone-rich Lower Member and the mudstone-rich Upper Member, we cannot distinguish the lithostratigraphic difference. Maeda (1957, 1961) correlated the Nobu-dani and Oyama Formations with the Kitadani Formation in the Takinami area, Katsuyama City, Fukui Prefecture (Fig.1). Kawai (1959), on the other hand, correlated the two formations with the Upper Cretaceous Asuwa Group.

Andesitic to dacitic dikes cut part of the Tetori Group and the Paleozoic basement, and the Hayashidani Andesite (Tanase et al., 1994; Wakita et al., 1992), striking east and dipping 30°–50°S, sporadically occurs on top of the Tetori Group. We interpret that the Hayashidani Andesite conformably covers the Tetori Group because the attitude of bedding of the two lithostratigraphic units is subparallel to each other, although we have not confirmed the contact between the two. The Omodani Rhyolite (Kawai, 1956, 1959), consisting of dacitic to rhyolitic lava and pyroclastic rocks, unconformably covers the Tetori Group and the Hayashidani Andesite. The Omodani Rhyolite strikes east and dips 10°–50°S.

Jinzu Region

Yamanomura area (Fig. 3)—The Yamanomura area is in the northern part of Hida City, Gifu Prefecture. Four members of the Tetori Group in the Jinzu Region make a conformable succession in this area; they are the Ioridanitoge Conglomerate and Inotani Alternation (Nakanomatanokkoshi Sandstone) Members of the Nagatogawa Formation, and Minamimatadani Conglomerate and Wasabu Alternation Members of the Atotsugawa Formation, in ascending order (Kawai and Nozawa, 1958; Harayama

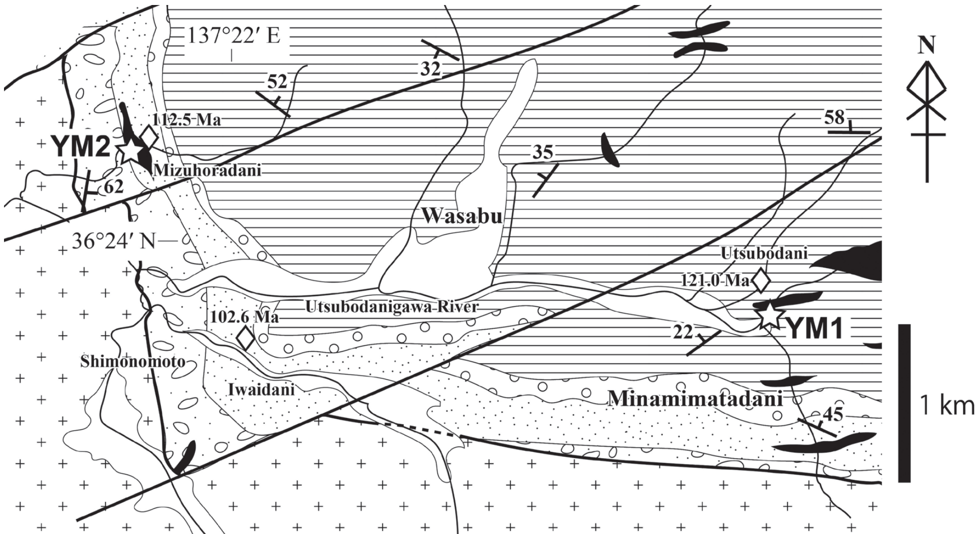

FIGURE 3. Geologic map of the Yamanomura area in the Jinzu Region. Modified after Gifu-ken Dinosaur Fossil Excavation Party (1997). Diamonds denote the sampling locations of zircons for the fission-track dating of Matsukawa et al. (2014a). Stars denote sampling locations of this study. Abbreviations—Alt.: Alternation, Cgl.: Conglomerate, Mb.: Member.

et al., 1991). The type localities for the Minamimatadani Conglomerate and Wasabu Alternation Members are in this area. The Ioridanitoge Conglomerate Member consists mainly of cobble to boulder conglomerate with some layers of fine to coarse feldspathic arenite. The cobbles and boulders of the conglomerate are mostly of granite, gneiss, and quartz porphyry (Kawai and Nozawa, 1958; Gifu-ken Dinosaur Fossil Excavation Party, 1997). The Inotani Alternation Member consists mostly of coarse arkosic sandstones interbedded with thinner shales and rare tuffaceous rocks (Kawai and Nozawa, 1958). The Minamimatadani Conglomerate Member consists of conglomerate and pebbly sandstone. The conglomerate contains pebbles and cobbles, of various rock types: felsic volcanic rocks, black mudstone, granite, gneiss, quartz porphyry, dark gray shale, arkosic granule sandstone, and chert. The Wasabu Alternation Member consists mostly of medium to coarse, bedded or massive feldspathic arenites interbedded with dark gray shales and rare conglomerates and tuffaceous rocks.

Many andesitic to rhyolitic dikes cut the Tetori Group in this area (Gifu-ken Dinosaur Fossil Excavation Party, 1997; Kawai and Nozawa, 1958). The dikes are mostly altered, and the surrounding rocks, including the Tetori Group, have suffered contact metamorphic effects.

Oyama area (Fig. 4)—The Oyama area of Toyama City is in the northwestern part of the Jinzu Region. In this area, there is a dinosaur-footprint site (Matsukawa et al., 1997; Hirasawa et al., 2010; Toyama Dinosaur Research Group, 2002) that also yields fossil dinosaur teeth. However, there is no unified view of the stratigraphic horizon of this remarkable site, because the Minamimatadani Conglomerate Member, separating the Inotani and Wasabu Alternation Members, thins out in this area. Yamada et al. (1988) and Hirasawa et al. (2010) placed the site in the Inotani and Wasabu Alternation Members, respectively, and Matsukawa et al. (2014a) lumped the two alternation members into the Inotani Formation of the Jinzu Group.

SAMPLE DESCRIPTIONS

Itoshiro-Oyama area in the Hakusan Region

Hayashidani Andesite (Fine tuff; Sample IO1)—Sample IO1 was collected from an outcrop of fine massive andesitic tuff along the Takigadani in Gujo City, Gifu Prefecture (35° 57′ 34.8″ N, 136° 45′ 4.0″ E; Fig. 2). The tuff consists of plagioclase, and opaque minerals, including alteration minerals such as chlorite (Fig. 5a). The tuff also contains devitrified glass replaced by chlorite or sericite and few lapilli. The lapilli have phenocrysts of plagioclase and clinopyroxene. The tuff grades upwards into cross-laminated, reddish purple tuffaceous sandstone.

Felsic dike (Sample IO2)—Sample IO2 was collected from an outcrop of a felsic dike along the Itoshirogawa River (35° 57′ 34.8″ N, 136° 45′ 28.6″ E; Fig. 2). The dike cuts the Nobu-dani Formation of the Tetori Group. Although the dike forms no evident metamorphic contact aureole, the Tetori Group in the vicinity of the dike is substantially hardened. Phenocrysts, mostly plagioclase, occupied 30 vol% of the sample (Fig. 5b). The other

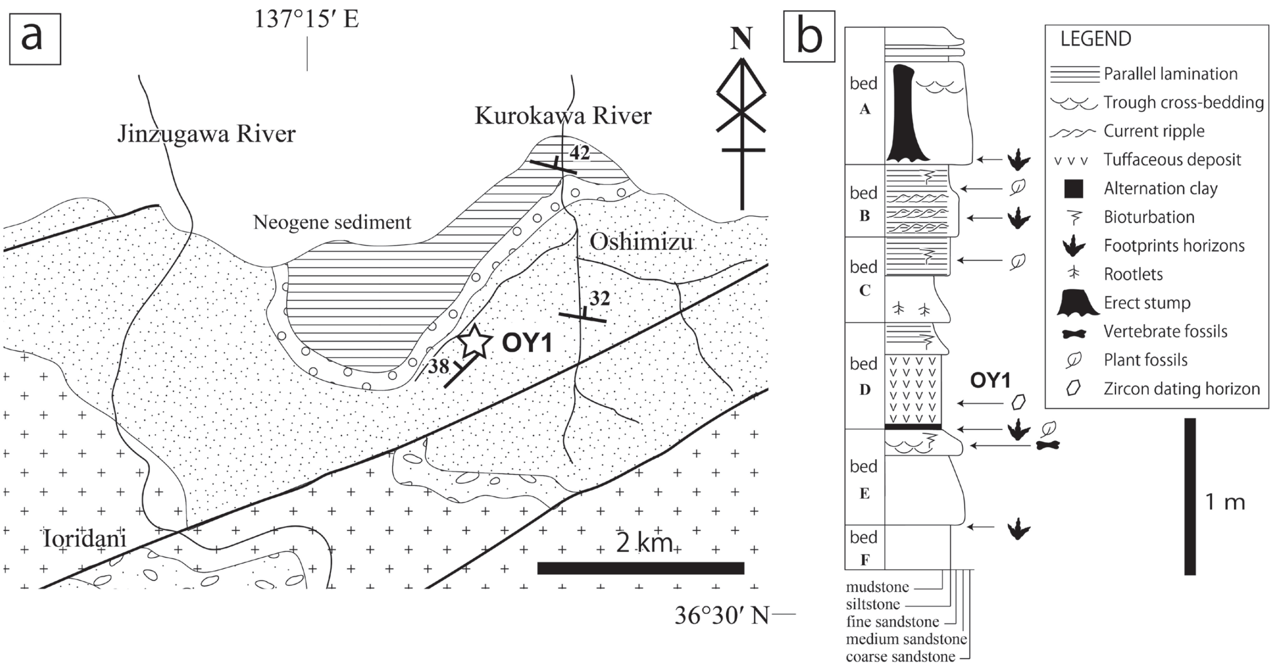

FIGURE 4. **a,** Geologic map of the Oyama area in the Jinzu Region modified after Yamada (1988). Keys are the same with those of Figure 3. The star denotes sampling location OY1 in this study. **b,** Columnar section of the dinosaur-footprint site modified after Hirasawa et al. (2010).

constituent minerals, including alteration minerals, were quartz, chlorite, and opaque minerals. Maeda (1957) described these dikes as quartz porphyries.

Jinzu Region

Felsic dike (Garnet dacite: Sample YM1)—Sample YM1 was collected from an outcrop of a felsic dike along the Utsubodanigawa River, Hida City, Gifu Prefecture (36° 23′ 42.59″ N, 137° 25′ 16.73″ E; Fig. 3). The dike cuts the Wasabu Alternation Member of the Tetori Group (*s.s.*). Although the dike forms no evident metamorphic contact aureole, the Tetori Group around the dike is partly bleached because of alteration. Gifu-ken Dinosaur Fossil Excavation Party (1996, 1997) has already reported the distribution of garnet-bearing felsic rocks near this location. Phenocrysts occupied 30 vol% of the sample, among which 90 vol% were quartz and plagioclase, and 10 vol% or less were garnet (Fig. 5c, d). The other constituent minerals, including alteration minerals, were chlorite and opaque minerals.

Felsic dike (Sample YM2)—Sample YM2 was collected from an outcrop of a felsic dike along the Mizuhoradani, Hida City, Gifu Prefecture (36° 24′ 18.35″ N, 137° 25′ 16.73″ E; Fig. 3). The felsic dike cut the Tetori Group and the basement Hida Granite (Gifu-ken Dinosaur Fossil Excavation Party, 1997). Although the dike forms no evident metamorphic contact aureole, the Tetori Group around the dike is partly bleached because of alteration. The constituent minerals, including alteration minerals, were quartz, plagioclase, biotite, chlorite, and opaque minerals (Fig. 5e). Matsukawa et al. (2014a) reported Albian zircon fission-track ages from tuffaceous sandstone samples taken near the location.

Tuff (Sample OY1)—Sample OY1 was collected from the tuff bed at Oyama dinosaur footprint site, southwestern Oshimizu, Toyama City (Toyama Dinosaur Research Group, 2002: 36° 31′ 43.70″ N, 137° 16′ 6.33″ E) just above the best-preserved footprint horizon (upper surface of Bed E; Fig. 4). The tuff consisted of quartz, plagioclase, biotite, and devitrified glass replaced by chlorite with the diameter of about 0.03 mm (Fig. 5f). The quartz crystals sometimes showed wavy extinction, and the plagioclase and biotite crystals displayed columnar or acicular euhedral form. Board of Education of Toyama Prefecture (2003) reported detailed description of the sample. Hirasawa et al. (2010) interpreted that the tuff is an ash-fall deposit.

ANALYTICAL METHOD

Zircon separates were prepared and analyzed following the procedures described in Kawagoe et al. (2012). A brief description of the analytical method is given below.

Zircon grains were separated from each sample and were mounted in acrylic resin and polished. The internal textures, solid phase inclusions, and microcracks of the zircons were observed using transmitted and reflected optical microscopy and monochromatic cathodoluminescence (CL) scanning electron microscope (SEM) imaging. CL images were captured on a JEOL JSM-5910LV SEM equipped with a JEOL MP-Z01118T CL detector in the Fukui Prefectural Dinosaur Museum. All zircon grains exhibit clear oscillatory zoning in CL images (Fig. 6). A portion of each grain, having no inclusions, microcracks, and

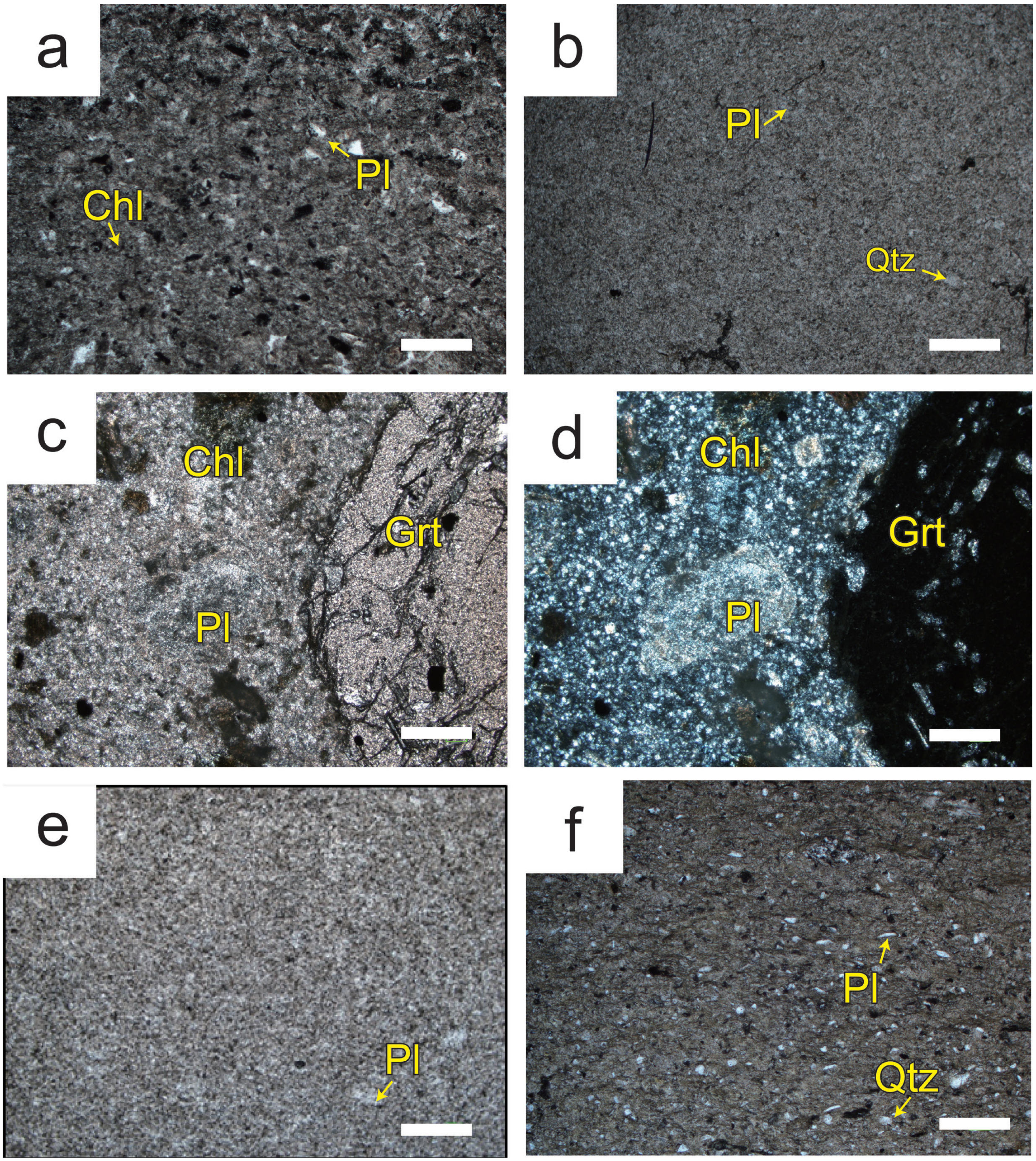

FIGURE 5. Photomicrographs of the studied samples (white scale bar = 300 μm). **a,** Fine tuff of the Hayashidani Andesite (open nicol; sample IO1) from the Itoshiro-Oyama area. **b,** Felsic dike from the Itoshiro-Oyama area (open nicol; sample IO2). **c–d,** Felsic dike (garnet dacite) from the Yamanomura area (sample YM1). **c**: open nicol, **d**: crossed nicols. **e,** Felsic dike from the Yamanomura area (open nicols; sample YM2). **f,** Fine tuff from the Oyama area (open nicols; sample OY1). Abbreviations—Chl: chlorite, Grt: garnet, Pl: plagioclase, Qtz: quartz.

detritus core, was chosen for analyses.

U-Pb dating was carried out on the laser ablation inductively coupled plasma mass spectrometer (LA-ICPMS) equipped in the Graduate School of Environmental Studies, Nagoya University. The ICPMS instrument was an Agilent 7700x quadrupole-based ICPMS connected with LA system (New Wave Research NWR-213), which used the frequency quintupled Nd-YAG 213-nm wavelength. NIST (National Institute of Standards and Technology, U.S.A.) SRM 610 glass with the recommended $^{206}Pb/^{238}U$ value of 0.2236 and the Nancy 91500 zircon with the

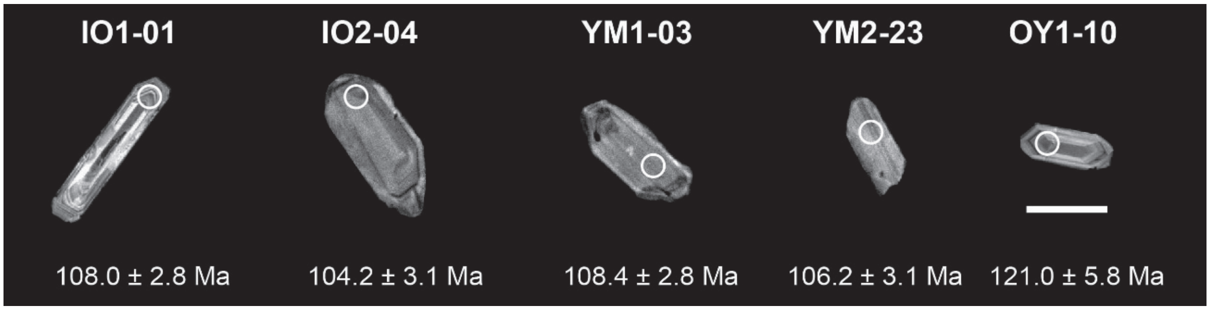

FIGURE 6. The cathodoluminescence image of a zircon grain from each sample. White circles denote the measurement spots (25 μm), and the numbers below denote the ^{238}U-^{206}Pb age of each spot. The scale bar is 100 μm.

TABLE 1. Analytical conditions and settings for zircon U-Pb dating. 2SD is the standard deviation of the standard glass isotopic ratio multiplied by 2.

Laser ablation system	Nagoya University (Based on Kouchi et al., 2015)				
Instrument	NWR-213 frequency quadrupled Nd-YAG laser (ESI, Portland, USA)				
Laser wave length	213 nm				
Laser energy	11.7 J cm^{-2}				
Repetition rate	10 Hz				
Crater size	25 μm				
Pre abration	8 s				
Ablation time	10 s				
Carrier gas (flow rate)	He (1.00 L min^{-1})				
ICPMS system					
Model	Agilent 7700x (Agilent Technologies, USA)				
Forward power	1400 W				
Monitor elements	^{202}Hg , ^{204}(Hg + Pb), ^{206}Pb,^{207}Pb, ^{208}Pb , ^{232}Th, ^{238}U				
Carrier gas (flow rate)	Ar (0.900–1.10 L min^{-1})				
Scan mode	Peak jump mode				
Detecer mode	Pulse counting				
Standard materials					
Standard glass	NIST 610 (^{206}Pb/^{238}U=0.2236 : Horn and von Blanckenburg, 2007)				
Standard zircon	Nancy 91500 (Wiedenbeck et al., 1995)				
Uncertainties and quality control	IO1	IO2	YM1	YM2	OY1
^{206}Pb/^{238}U (2SD)	1.5–2.7	1.3–2.2	1.4–2.2	1.4–2.5	2.0–3.2
^{207}Pb/^{206}Pb (2SD)	1.3–2.6	0.9–1.9	1.5–2.9	1.4–2.5	1.4–3.3
^{208}Pb /^{232}Th (2SD)	1.4–3.0	1.7–3.6	1.9–5.0	1.3–4.2	2.6–3.2
91500 zircon^{206}Pb/^{238}U age (n, MSWD)	1069 ± 48 Ma (3, 2.0)	1072 ± 15 Ma (3, 0.25)	1077 ± 35 Ma (3, 1.7)	1059 ± 15 Ma (3, 0.22)	1049 ± 19 Ma (3, 1.02)
91500 zircon^{207}Pb/^{206}Pb age (n, MSWD)	1081 ± 44 Ma (3, 1.4)	1058 ± 42 Ma (3, 0.14)	1035 ± 32 Ma (3, 1.9)	1085 ± 41 Ma (3, 0.69)	1071 ± 43 Ma (3, 2.2)

^{238}U-^{206}Pb age of 1062.4 ± 0.4 Ma (Wiedenbeck et al., 1995) were used as standard materials. The measurement conditions, given in Table 1, were based on a protocol by Kouchi et al. (2015): energy density of 11.7 J/cm^{-2}, pulse repetition rate of 10 Hz, pre-ablation time of 8 s, ablation time of 10 s, and the ablation pit size of 25 μm. The peaks of ^{202}Hg, ^{204}(Hg+Pb), ^{206}Pb, ^{207}Pb, ^{208}Pb, ^{232}Th, and ^{238}U were monitored. Data were acquired in sequences of 28 analyses, consisting of 5 analyses of gas blank, 4 NIST SRM 610 glass standard, one Nancy 91500 zircon, nine unknown, 4 SRM 610 standard, and five gas blank. Note that Kawagoe et al. (2012) and Takeuchi et al. (2015) also carried out zircon U-Pb dating with the same instruments and measurement conditions.

After the analyses, we rejected the following analytical data: (1) the data from a spot containing an inclusion or a crack, (2) the data from a zircon grain that leaped during laser ablation, and (3) the data with the amount of common lead (^{206}PbC; Stacey and Kramers, 1975) of 5% or more. We plotted all the remaining data on a concordia diagram using Isoplot 4.15 (Ludwig, 2012). Then we chose concordant spots (spots with concordant ^{238}U-^{206}Pb and ^{235}U-^{207}Pb data sets) with the error ellipse (2σ) overlapping the concordia line (Matsui et al., 2018). The slope of the ellipse is represented by the rho (ρ) value, the correlation coefficient of error in the $^{206}Pb/^{238}U$-$^{207}Pb/^{235}U$ ratios.

We defined the igneous age of each rock sample as follows. Since pyroclastic and volcanic rocks tend to contain older inherited and/or exotic zircons, we calculated the concordia age of several spots that form the youngest age cluster; i.e., the youngest spot and other spots with the error bar (2σ) of the ^{238}U-^{206}Pb age overlapping with that of the youngest spot. The data from inherited and exotic zircons, exhibiting significantly older ages, were eliminated from the calculation. We will mainly use the concordia age of concordant spots in the following description

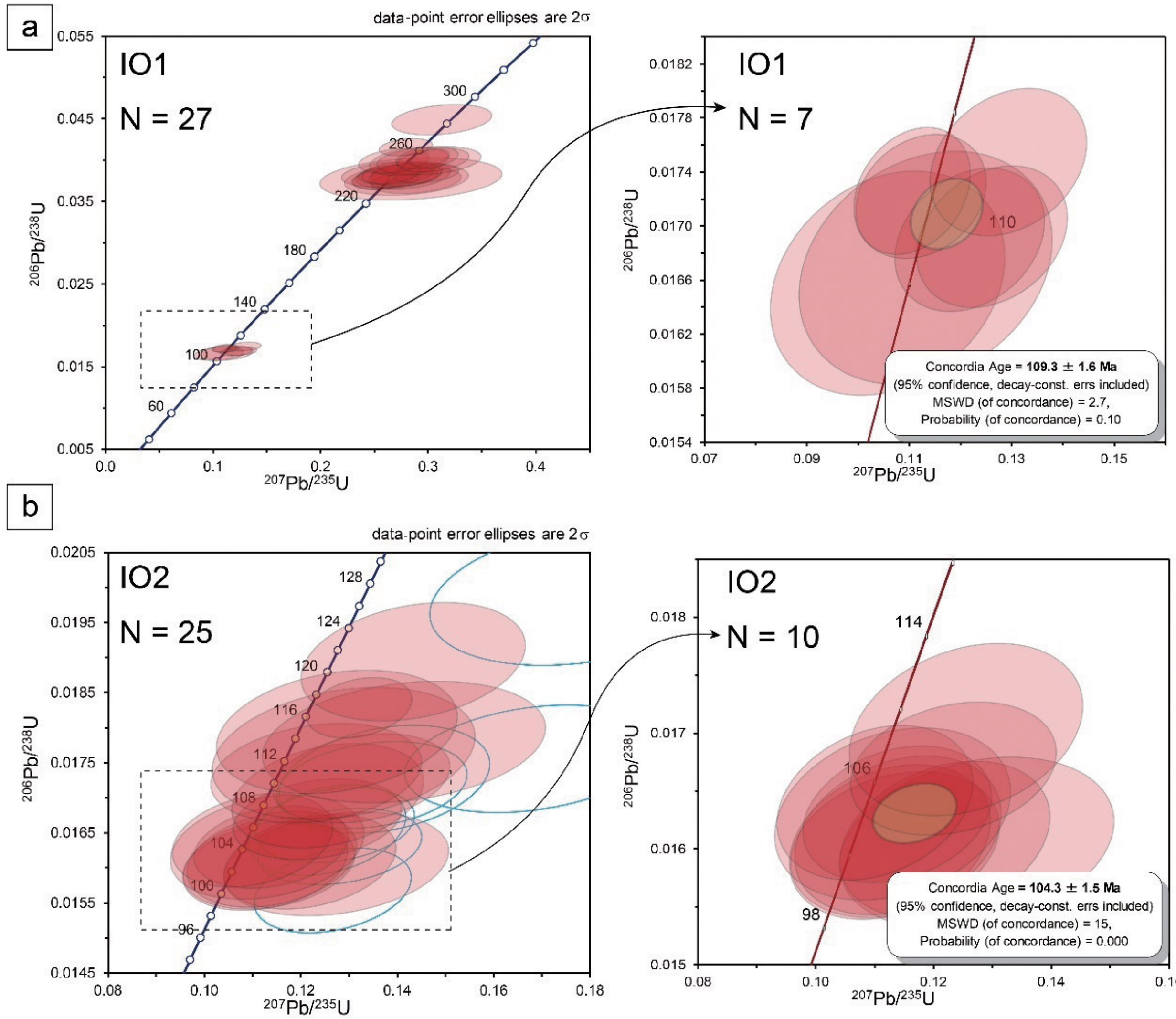

FIGURE 7. Analytical data of zircons from fine tuff and felsic dike of the Itoshiro-Oyama area of the Hakusan Region. **a,** Concordia diagram for all data (left) and the ^{238}U-^{206}Pb ages for seven concordant zircons forming the youngest cluster with the calculated concordia age (right) from fine tuff of the Hayashidani Andesite (sample IO1). **b,** Concordia diagram for all data (left) and the ^{238}U-^{206}Pb ages for ten concordant zircons forming the youngest cluster with the calculated concordia age (right) from a felsic dike (sample IO2). Blue open circles in the concordia diagrams in Figs. 7 and 8 show the analytical data for discordant spots. Abbreviations (Figs. 7 and 8)—N: total number, MSWD: mean standard weighted deviation.

and discussion. The age assignments to the geologic time scale in this study are based on International Commission for Stratigraphy (2018).

RESULTS

We conducted three cycles of measurements of zircons for each rock sample and calculated the following values for the zircon and glass standards. One is the weighted mean ^{238}U-^{206}Pb and ^{207}Pb-^{206}Pb age of the three spots on the Nancy 91500 standard zircon for each rock sample (Table 1). The others are percent relative standard deviations (%SD) of the ^{206}Pb/^{238}U, ^{207}Pb/^{206}Pb, and ^{208}Pb/^{232}Th ratios of eight spots on the SRM 610 standard for each cycle (%2SD in Table 1), a measure of repeatability of the measurements. The weighted mean ^{238}U-^{206}Pb ages of the Nancy 91500 zircon all gathered around its recommended age of 1062.4 ± 0.4 Ma within the range of error. The %2SD values of the ^{206}Pb/^{238}U, ^{207}Pb/^{206}Pb and ^{208}Pb/^{232}Th ratios of the SRM 610 glass were all below 5.0.

Hakusan Region

Andesitic tuff (Sample IO1)—We obtained analytical data from 27 spots in 27 zircon grains and adopted all the data sets (Table 2). Then we chose 27 concordant data sets out of 27 (Fig. 7). The ^{238}U-^{206}Pb ages of the concordant spots clustered in 106–

112 Ma and 238–283 Ma, and the ^{238}U-^{206}Pb age of the youngest concordant spot was 106.4 ± 4.3 Ma (2σ). The concordia age of the youngest cluster (7 spots) was 109.3 ± 1.6 Ma (MSWD = 2.7, probability = 0.10). The weighted mean of the ^{238}U-^{206}Pb ages of the youngest cluster was 109.3 ± 1.7 Ma (MSWD = 1.5, probability = 0.17) .

Felsic dike (Sample IO2)—We obtained analytical data from 27 spots in 27 zircon grains and adopted 25 data sets (Table 2). Then we chose 17 concordant data sets out of 25 (Fig. 6). The ^{238}U-^{206}Pb ages of the concordant spots clustered in 103–121 Ma, and the ^{238}U-^{206}Pb age of the youngest concordant spot was 102.6 ± 3.3 Ma. The concordia age of the youngest cluster (10 spots) was 104.3 ± 1.5 Ma (MSWD = 15, probability = 0.000). The weighted mean of the ^{238}U-^{206}Pb ages of the youngest cluster was 104.3 ± 1.4 Ma (MSWD = 1.5, probability = 0.17).

Jinzu Region

Felsic dike (Garnet dacite: Sample YM1)—We obtained analytical data from 27 spots in 27 zircon grains and adopted all the data sets (Table 2). Then we chose 20 concordant data sets out of 27 (Fig. 7). The ^{238}U-^{206}Pb ages of the concordant spots clustered in 107–121 Ma, and the ^{238}U-^{206}Pb age of the youngest concordant spot was 107.0 ± 3.1 Ma. The concordia age of the youngest cluster (14 spots) was 108.9 ± 0.7 Ma (MSWD = 7.6, probability = 0.006). The weighted mean of the ^{238}U-^{206}Pb ages of the youngest cluster was 108.9 ± 0.9 Ma (MSWD = 1.2, probability = 0.24).

Felsic dike (Sample YM2)—We obtained analytical data from 27 spots in 27 zircon grains and adopted all the data sets (Table 2). Then we chose 25 concordant data sets out of 27 (Fig. 7). The ^{238}U-^{206}Pb ages of the concordant spots clustered in 105–146 Ma, and the ^{238}U-^{206}Pb age of the youngest concordant spot was 105.4 ± 2.1 Ma. The concordia age of the youngest cluster (10 spots) was 106.9 ± 1.0 Ma (MSWD = 9.6, probability = 0.002). The weighted mean of the ^{238}U-^{206}Pb ages of the youngest cluster was 106.9 ± 0.8 Ma (MSWD = 0.89, probability = 0.54).

Fine tuff (Sample OY1)—We obtained analytical data from 27 spots in 27 zircon grains and adopted 25 data sets (Table 2). Then we chose 23 concordant data sets out of 25 (Fig. 7). The ^{238}U-^{206}Pb ages of the concordant spots clustered in 115–129 Ma and scattered at 209 and 251 Ma. The ^{238}U-^{206}Pb age of the youngest concordant spot was 115.5 ± 6.8 Ma. The concordia age of the youngest cluster (19 spots) was 120.9 ± 1.1 Ma (MSWD = 3.0, probability = 0.081). The weighted mean of the ^{238}U-^{206}Pb ages of the youngest cluster was 120.9 ± 1.1 Ma (MSWD = 1.01, probability = 0.44).

DISCUSSION

Igneous activity that terminated the deposition of the Tetori Group

We studied the zircon U-Pb ages of the andesitic tuff of the Hayashidani Andesite overlying the Tetori Group (*s.s.*) in the Itoshiro-Oyama area (IO1) and of felsic dikes cutting the Tetori Group (*s.s.*) in the Itoshiro-Oyama (IO2) and Yamanomura (YM1, YM2) areas. We interpret that the concordia ages of the youngest age-cluster of each sample is a measure of the consolidation age of the magma that formed each sample from the following reasons. (1) The closure temperature of the zircon U-Pb system, ca. 900 ℃ (Cherniak and Watson, 2000), lies between the temperatures of normal rhyolitic and basaltic magmas; and (2) normal life-span of an arc volcano is one million years or less, comparable to the error of the U–Pb dating of 100-million-year-old zircon grains. Thus, we suggest that the volcanic or pyroclastic rocks of samples IO1, IO2, YM1, and YM2 were formed at 109.3 ± 1.6 Ma, 104.3 ± 1.5 Ma, 108.9 ± 0.7 Ma, and 106.9 ± 1.0 Ma, respectively, in a middle Albian continuous igneous activity. Accordingly, we propose that the deposition of the Tetori Group (*s.s.*) in the Hakusan and Jinzu Regions terminated by ca. 104–109 Ma (middle Albian), which corresponds to the inferred numerical age of DS4 of Sano (2015).

Period of deposition of the Tetori Group in the Jinzu Region

The period of deposition of the Tetori Group (*s.s.*) in the Jinzu Region included ca.121 Ma (early Aptian) and terminated by 104–109 Ma (middle Albian). The concordia ages of the youngest zircon cluster from the OY1 tuff in the Jinzu Region was 120.9 ± 1.1 Ma. We interpret that this is the best measure of the age of deposition of the OY1 tuff as discussed in the previous section. Recently, Sakai et al. (2015) reported the zircon U-Pb age of 121.2 ± 1.1 Ma from a tuff sample of the Akaiwa Formation, a lithostratigraphic unit of DS3 of Sano (2015), of the Tetori Group in the Hakusan Region. The age of the tuff samples from the Jinzu and Hakusan Regions are concordant within error, indicating that terrestrial clastic rocks of DS3 with ca. 121 Ma tuff commonly occur in both the Jinzu and Hakusan Regions (Fig. 9).

Matsukawa et al. (2014a) interpreted that the Inotani Formation of the Jinzu Group (*sensu* Matsukawa et al., 2014a) was deposited in the Aptian–Albian or later because they obtained Aptian–Albian zircon fission-track ages from four tuffaceous sandstone samples of the formation. Three samples among the four were collected from the Yamanomura area, and their ages were 112.5, 102.6, and 121.0 Ma, in ascending order. The age of the uppermost sample was identical with the Aptian zircon U-Pb age of the OY1 tuff, whereas the ages of the lower two samples corresponded to the Albian. Maeda and Takenami (1957) and Gifu-ken Dinosaur Fossil Excavation Party (1997) have reported many dikes and sills, including the felsic dikes YM1 and YM2 we sampled, around the locations of the lower two tuffaceous sandstone samples. The zircon U-Pb ages of YM1 and YM2 are 108.9 ± 0.7 Ma and 106.9 ± 1.0 Ma, respectively, and lie between the two zircon fission-track ages of the lower tuffaceous sandstone samples. Considering (1) the irregular zircon fission-track ages concerning the stratigraphic horizons and (2) the relatively low closure temperature (ca. 250°C; Hurford, 1986), we suggest that these Albian fission-track ages are rejuvenation ages caused by

TABLE 2. U-Pb isotopic data for zircons analyzed in this study. Analyses shown in italics are discordant data sets. ^{206}PbC is the common lead composition.

Sample	^{235}U-^{207}Pb (Ma)	Error 2σ	^{238}U-^{206}Pb (Ma)	Error 2σ	^{206}PbC (%)	^{207}Pb/^{235}U	Error 2σ	^{206}Pb/^{238}U	Error 2σ	Th/U
Fine tuff (IO1) from the Hayashidani Andesite in the Itoshiro-Oyama area, Hakusan Region										
IO1-01	116.7	± 11.4	108.0	± 2.8	0.00	0.1218	± 0.0119	0.01690	± 0.00043	0.14
IO1-02	265.6	± 21.1	254.6	± 6.8	1.16	0.2990	± 0.0237	0.04029	± 0.00107	0.01
IO1-03	267.1	± 35.2	252.8	± 8.9	4.14	0.3009	± 0.0396	0.04000	± 0.00141	0.19
IO1-04	233.2	± 20.9	239.2	± 6.6	0.14	0.2582	± 0.0231	0.03780	± 0.00105	0.11
IO1-05	250.6	± 42.2	238.7	± 10.0	0.00	0.2799	± 0.0471	0.03772	± 0.00158	0.49
IO1-06	242.2	± 25.3	242.3	± 6.5	0.00	0.2694	± 0.0282	0.03830	± 0.00102	0.45
IO1-07	123.4	± 11.9	111.7	± 2.8	1.00	0.1293	± 0.0125	0.01748	± 0.00044	0.65
IO1-08	120.6	± 11.5	108.2	± 2.7	0.00	0.1261	± 0.0120	0.01692	± 0.00043	0.74
IO1-09	239.2	± 33.8	242.2	± 8.1	0.00	0.2656	± 0.0376	0.03829	± 0.00129	0.37
IO1-10	250.0	± 18.2	262.7	± 5.5	0.00	0.2792	± 0.0203	0.04159	± 0.00087	0.94
IO1-11	254.0	± 61.8	239.1	± 13.3	0.00	0.2842	± 0.0692	0.03779	± 0.00209	0.35
IO1-12	243.4	± 28.1	240.6	± 7.1	0.00	0.2708	± 0.0313	0.03803	± 0.00112	0.28
IO1-13	106.4	± 8.9	110.3	± 2.4	1.07	0.1105	± 0.0093	0.01726	± 0.00038	0.10
IO1-14	264.4	± 22.6	243.3	± 6.1	2.33	0.2975	± 0.0255	0.03846	± 0.00096	0.43
IO1-15	241.2	± 23.8	252.5	± 7.6	0.53	0.2681	± 0.0265	0.03995	± 0.00120	0.39
IO1-16	239.1	± 20.1	243.3	± 6.8	0.00	0.2655	± 0.0223	0.03846	± 0.00108	0.46
IO1-17	276.3	± 33.5	283.2	± 9.5	2.35	0.3128	± 0.0379	0.04491	± 0.00151	0.80
IO1-18	257.7	± 30.4	237.5	± 8.1	0.00	0.2889	± 0.0341	0.03753	± 0.00128	0.65
IO1-19	270.1	± 24.2	253.2	± 7.4	0.16	0.3048	± 0.0273	0.04007	± 0.00117	0.11
IO1-20	250.6	± 24.4	242.3	± 7.3	0.57	0.2800	± 0.0273	0.03831	± 0.00116	0.22
IO1-21	102.0	± 18.0	106.0	± 4.3	4.62	0.1057	± 0.0187	0.01658	± 0.00068	0.52
IO1-22	108.8	± 19.4	106.7	± 4.5	2.69	0.1131	± 0.0202	0.01669	± 0.00070	0.62
IO1-23	235.1	± 23.6	239.1	± 6.8	3.21	0.2606	± 0.0261	0.03778	± 0.00108	0.41
IO1-24	267.7	± 13.2	254.6	± 5.5	0.41	0.3017	± 0.0148	0.04028	± 0.00088	0.40
IO1-25	252.7	± 27.9	241.4	± 8.6	0.11	0.2826	± 0.0312	0.03815	± 0.00136	0.34
IO1-26	252.6	± 26.9	251.9	± 8.7	0.00	0.2824	± 0.0300	0.03984	± 0.00138	0.17
IO1-27	108.0	± 10.0	110.1	± 2.4	0.00	0.1122	± 0.0104	0.01722	± 0.00037	0.36
Felsic dike (IO2) in the Itoshiro-Oyama area, Hakusan Region										
IO2-02	*157.6*	*± 20.3*	*112.2*	*± 4.0*	*0.00*	*0.1680*	*± 0.0217*	*0.01756*	*± 0.00063*	*0.32*
IO2-03	126.4	± 14.3	110.4	± 3.3	0.58	0.1326	± 0.0150	0.01728	± 0.00052	0.39
IO2-04	109.5	± 12.6	104.2	± 3.1	4.70	0.1138	± 0.0131	0.01630	± 0.00048	0.27
IO2-05	109.1	± 14.0	102.6	± 3.3	0.00	0.1135	± 0.0145	0.01604	± 0.00051	0.30
IO2-06	121.7	± 18.2	102.6	± 3.9	0.00	0.1273	± 0.0191	0.01605	± 0.00061	0.28
IO2-07	*121.4*	*± 12.8*	*106.2*	*± 2.8*	*0.08*	*0.1271*	*± 0.0134*	*0.01661*	*± 0.00044*	*0.86*

Sample	^{235}U-^{207}Pb (Ma)	Error 2σ	^{238}U-^{206}Pb (Ma)	Error 2σ	^{206}PbC (%)	$^{207}Pb/^{235}U$	Error 2σ	$^{206}Pb/^{238}U$	Error 2σ	Th/U
IO2-08	118.0	± 17.1	110.9	± 3.7	0.87	0.1233	± 0.0179	0.01736	± 0.00058	0.33
IO2-09	*122.3*	*± 13.3*	*104.3*	*± 2.8*	*3.39*	*0.1280*	*± 0.0139*	*0.01630*	*± 0.00044*	*0.35*
IO2-10	*128.3*	*± 15.4*	*109.8*	*± 3.2*	*2.48*	*0.1347*	*± 0.0161*	*0.01718*	*± 0.00051*	*0.32*
IO2-11	134.3	± 22.8	113.7	± 4.5	1.63	0.1414	± 0.0240	0.01780	± 0.00071	0.26
IO2-12	118.2	± 13.7	106.7	± 3.0	3.97	0.1234	± 0.0143	0.01670	± 0.00047	0.46
IO2-13	126.0	± 8.5	116.8	± 2.2	1.09	0.1322	± 0.0089	0.01829	± 0.00035	0.61
IO2-14	*130.6*	*± 17.0*	*110.3*	*± 4.0*	*0.00*	*0.1373*	*± 0.0179*	*0.01727*	*± 0.00063*	*0.24*
IO2-15	116.8	± 14.0	102.9	± 3.5	0.00	0.1219	± 0.0146	0.01609	± 0.00055	0.39
IO2-16	*167.4*	*± 24.8*	*127.1*	*± 5.3*	*1.39*	*0.1792*	*± 0.0265*	*0.01991*	*± 0.00083*	*0.34*
IO2-17	123.0	± 21.3	112.7	± 4.9	0.00	0.1288	± 0.0223	0.01764	± 0.00077	0.32
IO2-18	109.6	± 13.8	103.1	± 3.6	0.51	0.1140	± 0.0143	0.01612	± 0.00056	0.30
IO2-19	*120.0*	*± 12.7*	*105.7*	*± 3.4*	*0.00*	*0.1255*	*± 0.0133*	*0.01654*	*± 0.00053*	*0.39*
IO2-21	136.0	± 18.0	121.0	± 4.4	1.86	0.1433	± 0.0190	0.01895	± 0.00069	1.31
IO2-22	*120.1*	*± 15.5*	*108.9*	*± 3.9*	*0.00*	*0.1255*	*± 0.0162*	*0.01703*	*± 0.00061*	*0.42*
IO2-23	*121.1*	*± 12.7*	*100.3*	*± 3.2*	*3.17*	*0.1267*	*± 0.0133*	*0.01568*	*± 0.00050*	*0.33*
IO2-24	121.9	± 19.5	114.7	± 4.6	1.75	0.1275	± 0.0204	0.01794	± 0.00072	0.45
IO2-25	106.0	± 13.1	104.9	± 3.5	2.50	0.1100	± 0.0136	0.01640	± 0.00054	0.32
IO2-26	108.3	± 13.4	102.7	± 3.5	0.00	0.1126	± 0.0139	0.01606	± 0.00054	0.27
IO2-27	108.7	± 15.8	104.3	± 3.9	0.00	0.1130	± 0.0164	0.01631	± 0.00061	0.52
Felsic dike (YM1) in the Yamanomura area, Jinzu Region										
YM1-01	*126.8*	*± 10.7*	*109.7*	*± 2.8*	*1.83*	*0.1331*	*± 0.0112*	*0.01716*	*± 0.00044*	*0.46*
YM1-02	107.5	± 9.1	113.6	± 2.8	0.09	0.1117	± 0.0094	0.01777	± 0.00043	0.51
YM1-03	108.8	± 10.2	108.4	± 2.8	0.00	0.1131	± 0.0106	0.01696	± 0.00044	0.45
YM1-04	111.2	± 13.6	108.1	± 3.4	2.23	0.1158	± 0.0142	0.01691	± 0.00053	0.32
YM1-05	*139.9*	*± 12.9*	*117.2*	*± 3.2*	*2.20*	*0.1477*	*± 0.0136*	*0.01835*	*± 0.00050*	*0.42*
YM1-06	105.0	± 10.2	111.2	± 2.9	0.00	0.1089	± 0.0106	0.01741	± 0.00046	0.46
YM1-07	109.5	± 9.4	111.3	± 2.8	0.70	0.1138	± 0.0097	0.01742	± 0.00043	0.41
YM1-08	132.1	± 12.4	121.3	± 2.8	1.52	0.1390	± 0.0131	0.01899	± 0.00044	0.46
YM1-09	111.4	± 10.3	107.7	± 2.4	2.75	0.1160	± 0.0107	0.01684	± 0.00038	0.43
YM1-10	109.9	± 11.5	107.6	± 2.6	2.67	0.1143	± 0.0119	0.01683	± 0.00041	0.45
YM1-11	109.3	± 10.8	109.7	± 2.6	1.96	0.1137	± 0.0113	0.01716	± 0.00040	0.48
YM1-12	118.1	± 16.7	117.5	± 3.7	0.00	0.1234	± 0.0175	0.01839	± 0.00058	0.33
YM1-13	108.5	± 10.7	107.0	± 3.1	0.08	0.1128	± 0.0111	0.01674	± 0.00049	0.52
YM1-14	*126.9*	*± 11.6*	*105.0*	*± 3.1*	*2.65*	*0.1331*	*± 0.0121*	*0.01643*	*± 0.00048*	*0.35*
YM1-15	118.3	± 12.0	111.8	± 3.3	0.00	0.1236	± 0.0125	0.01750	± 0.00052	0.39
YM1-16	114.7	± 11.4	113.6	± 3.3	0.00	0.1196	± 0.0119	0.01777	± 0.00052	0.42

Sample	^{235}U-^{207}Pb (Ma)	Error 2σ	^{238}U-^{206}Pb (Ma)	Error 2σ	^{206}PbC (%)	$^{207}Pb/^{235}U$	Error 2σ	$^{206}Pb/^{238}U$	Error 2σ	Th/U
YM1-17	*133.7*	*± 15.6*	*112.9*	*± 3.8*	*0.00*	*0.1408*	*± 0.0165*	*0.01767*	*± 0.00059*	*0.33*
YM1-18	119.6	± 10.1	108.4	± 3.0	1.56	0.1250	± 0.0106	0.01696	± 0.00047	0.56
YM1-19	117.8	± 9.3	107.7	± 2.2	1.26	0.1230	± 0.0097	0.01685	± 0.00035	0.60
YM1-20	113.6	± 9.6	112.9	± 2.4	2.15	0.1183	± 0.0100	0.01767	± 0.00037	0.46
YM1-21	*129.6*	*± 12.1*	*111.1*	*± 2.6*	*1.10*	*0.1362*	*± 0.0127*	*0.01738*	*± 0.00041*	*0.43*
YM1-22	*139.7*	*± 12.8*	*114.2*	*± 2.8*	*1.50*	*0.1475*	*± 0.0135*	*0.01787*	*± 0.00044*	*0.38*
YM1-23	117.6	± 10.1	109.8	± 2.5	0.83	0.1228	± 0.0105	0.01718	± 0.00039	0.45
YM1-24	*130.5*	*± 12.1*	*112.8*	*± 2.3*	*1.88*	*0.1371*	*± 0.0127*	*0.01765*	*± 0.00036*	*0.45*
YM1-25	114.8	± 10.6	107.9	± 2.1	2.97	0.1197	± 0.0111	0.01688	± 0.00033	0.43
YM1-26	119.9	± 10.2	113.0	± 2.0	0.00	0.1254	± 0.0107	0.01768	± 0.00032	0.48
YM1-27	115.2	± 13.5	110.0	± 2.7	1.72	0.1202	± 0.0141	0.01721	± 0.00043	0.32

Felsic dike (YM2) in the Yamanomura area, Jinzu Region										
YM2-01	139.8	± 5.8	139.7	± 2.5	0.06	0.1476	± 0.0062	0.02190	± 0.00039	0.42
YM2-02	133.4	± 5.7	134.2	± 2.4	0.00	0.1404	± 0.0060	0.02104	± 0.00038	0.44
YM2-03	*134.0*	*± 5.6*	*108.0*	*± 2.0*	*1.47*	*0.1411*	*± 0.0059*	*0.01690*	*± 0.00031*	*0.30*
YM2-04	133.3	± 5.1	134.2	± 2.4	0.00	0.1403	± 0.0053	0.02104	± 0.00038	0.44
YM2-05	139.1	± 5.3	137.8	± 2.1	0.33	0.1469	± 0.0056	0.02160	± 0.00033	0.41
YM2-06	104.2	± 6.0	107.3	± 2.4	0.43	0.1081	± 0.0063	0.01678	± 0.00037	0.16
YM2-07	128.2	± 5.2	128.9	± 2.7	0.18	0.1346	± 0.0055	0.02020	± 0.00042	0.43
YM2-08	*128.7*	*± 6.0*	*108.0*	*± 2.3*	*0.00*	*0.1351*	*± 0.0063*	*0.01690*	*± 0.00036*	*0.15*
YM2-09	142.2	± 4.9	141.7	± 2.4	0.14	0.1503	± 0.0051	0.02222	± 0.00037	0.50
YM2-10	145.0	± 5.7	146.3	± 2.5	0.13	0.1535	± 0.0061	0.02295	± 0.00040	0.24
YM2-11	140.8	± 5.2	141.6	± 2.4	0.05	0.1488	± 0.0055	0.02221	± 0.00038	0.42
YM2-12	113.4	± 5.2	109.4	± 2.4	0.39	0.1182	± 0.0054	0.01712	± 0.00037	0.20
YM2-13	112.7	± 5.1	111.8	± 2.2	0.41	0.1174	± 0.0053	0.01749	± 0.00035	0.16
YM2-14	108.1	± 4.9	105.4	± 2.1	0.24	0.1124	± 0.0051	0.01649	± 0.00033	0.16
YM2-15	110.8	± 5.1	111.8	± 2.2	0.38	0.1153	± 0.0053	0.01749	± 0.00035	0.24
YM2-16	110.2	± 6.2	107.1	± 2.8	0.38	0.1146	± 0.0064	0.01675	± 0.00044	0.15
YM2-17	106.6	± 5.3	105.8	± 2.7	0.45	0.1107	± 0.0055	0.01655	± 0.00042	0.18
YM2-18	111.4	± 5.7	106.8	± 2.8	0.44	0.1160	± 0.0059	0.01670	± 0.00043	0.23
YM2-19	112.3	± 5.3	106.9	± 2.7	0.68	0.1170	± 0.0055	0.01672	± 0.00042	0.30
YM2-20	110.9	± 5.3	111.7	± 2.8	0.08	0.1154	± 0.0056	0.01748	± 0.00043	0.16
YM2-21	134.6	± 6.2	135.8	± 3.4	0.06	0.1418	± 0.0066	0.02129	± 0.00053	0.30
YM2-22	112.3	± 5.8	106.3	± 2.7	0.23	0.1169	± 0.0061	0.01663	± 0.00042	0.14
YM2-23	105.3	± 5.4	106.2	± 3.1	0.21	0.1093	± 0.0056	0.01662	± 0.00048	0.16
YM2-24	133.1	± 5.4	132.0	± 3.7	0.13	0.1401	± 0.0057	0.02068	± 0.00058	0.50

Sample	^{235}U-^{207}Pb (Ma)	Error 2σ	^{238}U-^{206}Pb (Ma)	Error 2σ	^{206}PbC (%)	^{207}Pb/^{235}U	Error 2σ	^{206}Pb/^{238}U	Error 2σ	Th/U
YM2-25	132.8	± 4.9	131.6	± 2.0	0.00	0.1398	± 0.0052	0.02062	± 0.00031	0.31
YM2-26	135.2	± 5.1	135.8	± 2.0	0.18	0.1424	± 0.0054	0.02128	± 0.00032	0.34
YM2-27	106.8	± 4.7	107.3	± 1.7	0.00	0.1109	± 0.0049	0.01678	± 0.00026	0.20
Fine tuff (OY1) in the Oyama area, Jinzu Region										
OY1-01	126.5	± 22.9	119.7	± 7.3	3.01	0.1326	± 0.0240	0.01874	± 0.00115	0.98
OY1-02	123.8	± 18.2	117.8	± 6.8	1.00	0.1297	± 0.0191	0.01845	± 0.00106	0.61
OY1-03	116.3	± 12.9	118.0	± 6.3	0.00	0.1214	± 0.0134	0.01847	± 0.00099	0.52
OY1-04	*134.6*	*± 11.8*	*121.4*	*± 6.3*	*0.00*	*0.1417*	*± 0.0124*	*0.01901*	*± 0.00099*	*0.56*
OY1-05	126.9	± 16.9	118.5	± 6.7	0.00	0.1331	± 0.0177	0.01856	± 0.00104	0.90
OY1-07	124.0	± 18.6	121.1	± 7.0	0.00	0.1298	± 0.0195	0.01896	± 0.00109	0.62
OY1-08	244.0	± 26.5	251.3	± 13.5	0.13	0.2716	± 0.0295	0.03975	± 0.00214	0.72
OY1-09	128.8	± 19.9	115.5	± 6.8	1.99	0.1353	± 0.0209	0.01808	± 0.00106	0.40
OY1-10	110.8	± 19.9	121.0	± 5.8	1.46	0.1153	± 0.0207	0.01895	± 0.00090	0.63
OY1-12	204.3	± 24.0	208.9	± 8.3	0.00	0.2229	± 0.0262	0.03293	± 0.00131	1.22
OY1-13	128.9	± 14.0	119.8	± 4.6	0.00	0.1353	± 0.0147	0.01875	± 0.00073	0.66
OY1-14	132.0	± 18.9	121.0	± 5.3	0.00	0.1388	± 0.0198	0.01895	± 0.00083	0.62
OY1-15	122.3	± 14.0	116.1	± 4.6	0.00	0.1280	± 0.0146	0.01818	± 0.00071	0.73
OY1-16	118.9	± 16.0	119.2	± 5.0	0.00	0.1242	± 0.0168	0.01867	± 0.00078	0.52
OY1-17	122.3	± 20.1	120.1	± 5.6	2.37	0.1280	± 0.0211	0.01880	± 0.00087	0.69
OY1-18	119.1	± 15.9	120.9	± 4.0	3.05	0.1245	± 0.0166	0.01892	± 0.00063	0.60
OY1-19	125.1	± 7.6	123.4	± 2.8	0.00	0.1312	± 0.0080	0.01932	± 0.00044	0.60
OY1-20	119.1	± 16.9	124.7	± 4.3	0.87	0.1244	± 0.0176	0.01954	± 0.00067	0.60
OY1-21	127.4	± 12.2	125.6	± 3.5	0.00	0.1337	± 0.0128	0.01968	± 0.00055	0.69
OY1-22	119.7	± 14.0	123.3	± 3.8	1.11	0.1252	± 0.0147	0.01931	± 0.00059	0.55
OY1-23	122.5	± 10.4	120.4	± 3.1	1.54	0.1282	± 0.0109	0.01886	± 0.00049	0.91
OY1-24	*239.6*	*± 21.6*	*127.9*	*± 4.3*	*4.98*	*0.2662*	*± 0.0240*	*0.02004*	*± 0.00067*	*1.48*
OY1-25	129.6	± 22.3	121.8	± 5.3	0.00	0.1362	± 0.0234	0.01907	± 0.00082	0.95
OY1-26	127.2	± 16.0	121.8	± 4.3	1.31	0.1335	± 0.0168	0.01907	± 0.00067	0.70
OY1-27	145.4	± 26.1	128.5	± 5.9	0.00	0.1539	± 0.0277	0.02013	± 0.00092	0.78

the heating from ca. 104–109 Ma intrusive rocks. Matsukawa et al. (2014a) also reported an Albian zircon fission-track age from a tuffaceous sandstone sample of the Nagatogawa area, where intrusive rock bodies also occur (Maeda and Takenami, 1957; Matsukawa et al., 2014a, b; Shigeno, 2003). Although we have not obtained a zircon U-Pb age of the intrusive rocks in the Nagatogawa area, we suppose that the Albian zircon fission-track age would also be an annealed age. In conclusion, the Tetori Group (*s.s.*) in the Hakusan and Jinzu Regions commonly includes terrestrial sedimentary rocks of DS3 (*sensu* Sano, 2015) with 121 Ma (early Aptian) tuff. The fact does not support the idea of Matsukawa et al. (2014a) that the age of the Tetori Group (*s.s.*) in the Hakusan Region and Jinzu Region (Jinzu Group *sensu* Matsukawa et al., 2014a) differs from each other.

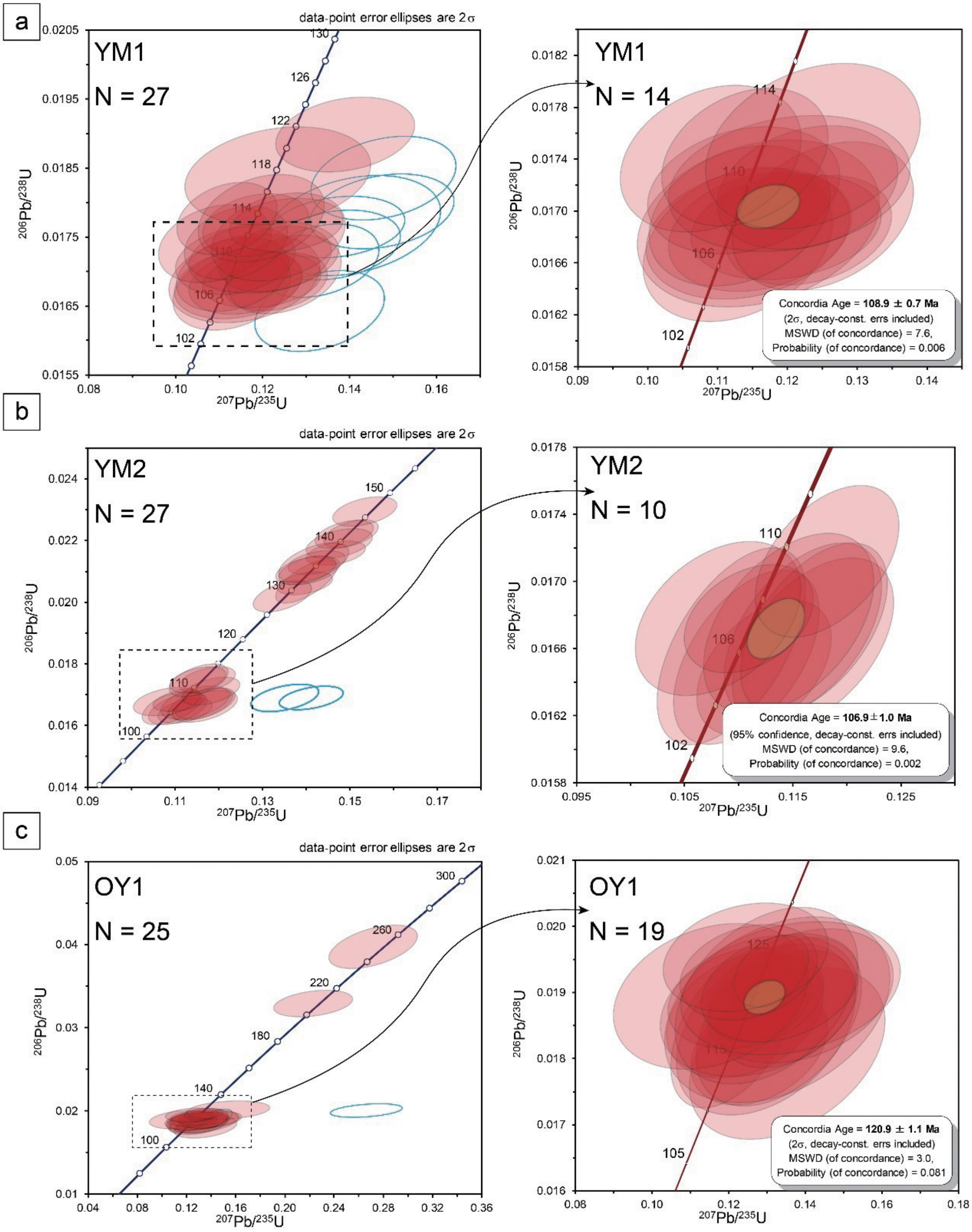

FIGURE 8. Analytical data of zircons from the felsic dike and fine tuff the Jinzu Region. **a,** Concordia diagram for all data (left) and the ^{238}U-^{206}Pb ages for fourteen concordant zircons forming the youngest cluster with the calculated concordia age (right) of a felsic dike (garnet dacite) in Yamanomura area (sample YM1). **b,** Concordia diagram for all data (left) and the ^{238}U-^{206}Pb ages for ten concordant zircons forming the youngest cluster with the calculated concordia age (right) from a felsic dike (sample YM2). **c,** Concordia diagram for all data (left) and the ^{238}U-^{206}Pb ages for nineteen concordant zircons forming the youngest cluster with the calculated concordia age (right) from fine tuff in the Oyama area (sample OY1).

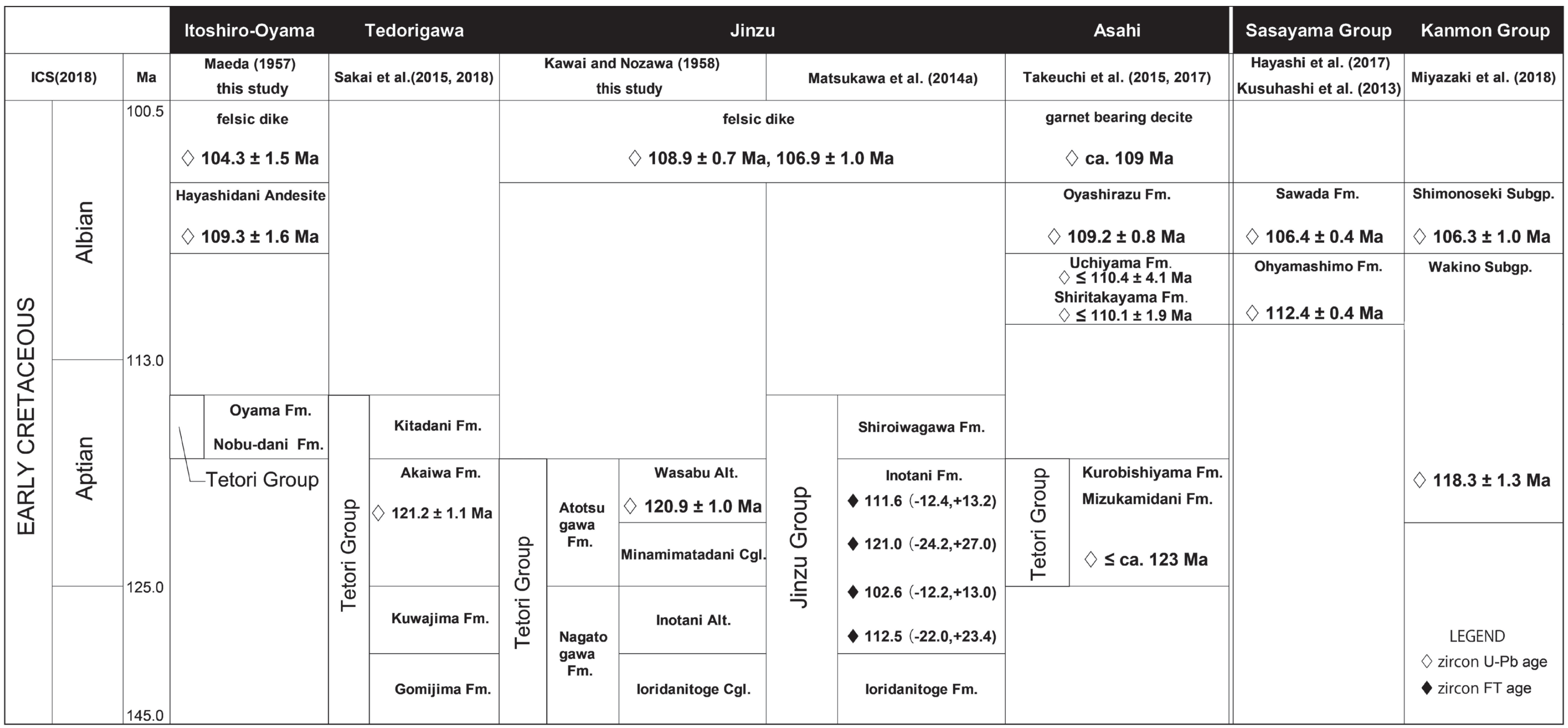

FIGURE 9. Stratigraphy and correlation of the Early Cretaceous in the Inner Zone of Southwest Japan. Abbreviations—Alt.: Alternation Member, Cgl.: Conglomerate Member, Fm.: Formation, Subgp.: Subgroup

Commencement of Early Cretaceous igneous activity in central and Southwest Japan

Takeuchi et al. (2015, 2017) already reported concordant data with us. Takeuchi et al. (2015) studied the U-Pb age of detrital zircons from the Mizukamidani Formation of the Tetori Group and that of the garnet dacite dike cutting the Tetori Group in the Asahi area, eastern Toyama Prefecture (Fig. 1). They obtained a cluster age of 123 Ma from the Mizukamidani Formation and that of 109 Ma from the garnet dacite dike. Thus they concluded that the Tetori Group in the Asahi area continued its deposition until 123 Ma or later, but cut by the dike of 109 Ma. Moreover, Takeuchi et al. (2017) reported the zircon U-Pb age of 109.2 ± 0.8 Ma from a welded-tuff sample of the Oyashirazu Formation that overlies the Tetori Group in the Asahi area and consists of andesitic to dacitic volcanic rocks. The ages of the Oyashirazu Formation and the Hayashidani Andesite (109.3 ± 1.6 Ma; this study) are concordant within error.

Andesitic to rhyolitic volcanic or pyroclastic rocks have also been reported from the Inner Zone of Southwest Japan. Kusuhashi et al. (2013) reported the zircon U-Pb age of 106.4 ± 0.4 Ma from the andesite of the Sawada Formation of the Sasayama Group (Hayashi et al., 2017) in Hyogo Prefecture. The Kisa Andesite in Hiroshima Prefecture and associated rhyolitic tuff yield the zircon U-Pb ages of 111.5 ± 1.5 Ma and 111.8 ± 0.9 Ma, respectively (Hayasaka et al., 2016). The rhyolitic tuff of the Shimonoseki Subgroup of the Kanmon Group in Yamaguchi Prefecture yields the zircon U-Pb age of 106.4 ± 1.0 Ma (Miyazaki et al., 2018). It is noteworthy that the Kanmon and Sasayama Groups both consist of fluvial clastic rocks covered with andesitic to rhyolitic volcanic and pyroclastic rocks and indicate a similar environmental change with that of DS3 (fluvial)–DS4 (volcanic) of Sano (2015). In the present-day Inner Zone of Southwest Japan, andesitic to rhyolitic igneous activity seems to have regionally commenced at ca. 104–112 Ma. Stratigraphy and correlation of the Early Cretaceous in the Inner Zone of Southwest Japan are summarized in Fig. 9.

CONCLUSIONS

We obtained LA-ICPMS U-Pb ages of igneous zircons from (1) a tuff sample of the Hayashidani Andesite of DS4 (Sano, 2015) that covers the Tetori Group (*s.s.*) in the Hakusan Region, (2) felsic dikes that cut the Tetori Group (*s.s.*) in the Hakusan and Jinzu Regions, and (3) a tuff sample (OY1) in the Tetori Group (*s.s.*) in the Jinzu Region. The results of the study and their implications can be summarized as follows.

1. The depositional age of the tuff of the Hayashidani Andesite was 109.3 ± 1.6 Ma, whereas the ages of the felsic dikes in the Hakusan and Jinzu Regions were 104.3 ± 1.5 Ma, 108.9 ± 0.7 Ma, and 106.9 ± 1.0 Ma. These DS4 ages strongly suggest that the deposition of the Tetori Group (*s.s.*) terminated by 104–109 Ma. Albian zircon fission-track ages from the Tetori Group (*s.s.*) of Matsukawa et al. (2014a), supporting their idea that the Tetori Group (*s.s.*) in the Jinzu Region (Jinzu Group *sensu* Matsukawa et al., 2014a) is of Aptian–Albian or younger age, are likely rejuvenation ages caused by the heating from the 104–109 Ma felsic dikes.
2. The depositional age of the OY1 tuff in the Tetori Group (*s.s.*) of the Jinzu Region was 120.9 ± 1.1 Ma and is identical with that of a tuff sample in the Akaiwa Formation (DS3) of Hakusan Region (121.2 ± 1.1 Ma; Sakai et al., 2015). These ages suggest that terrestrial clastic rocks of DS3 with ca.121 Ma tuff commonly occur both in the Hakusan and Jinzu Regions.

ACKNOWLEDGMENTS

We would like to express our sincere gratitude to Professor Shin-ichi Sano of the University of Toyama for various discussions and instructions during the course of this study. We thank Dr. Kazuhiro Miyazaki and Dr. Daisuke Sato of the Geological Survey of Japan, AIST for giving us advice on Cretaceous igneous activity in Southwest Japan. Critical reviews of the submitted manuscript by Emeritus Professor Kenji Konishi of Kanazawa University, Professor Toshihiro Yamada of Osaka City University, Tatsuki Tsujimori of Tohoku University, and Dr. Soichiro Kawabe of the Fukui Prefectural Dinosaur Museum are greatly appreciated. This study was supported by JSPS KAKENHI Grant Number 17K05746.

REFERENCES

Board of Education of Toyama Prefecture. 2003. Report of the Geological Survey of the Tetori Group in Toyama Prefecture. Board of Education of Toyama Prefecture, Toyama, 109 p.*

Cherniak, D. J., and E. B. Watson. 2000. Pb diffusion in zircon. Chemical Geology 172: 5–24.

Gifu-ken Dinosaur Fossil Excavation Party. 1996. Geology of the Tetori Group in the Kitanomatagawa area, Kamioka-cho, Gifu Prefecture, central Japan. Bulletin of the Gifu Prefectural Museum 17: 1–14.*

Gifu-ken Dinosaur Fossil Excavation Party. 1997. Geology of the Tetori Group in the Yamanomura area, Kamioka-cho, Gifu Prefecture, central Japan. Bulletin of the Gifu Prefectural Museum 18: 1–9.*

Harayama, S., M. Takeuchi, S. Nakano, T. Sato and F. Takizawa. 1991. Geology of the Yarigatake District with Geological Sheet Map at 1:50,000. Geological Survey of Japan, 190 pp.**

Hayasaka, Y., and S. Tashima. 2016. Late Cretaceous igneous activity and erosion history of Sanyo-Ryoke Province constrained by zircon U-Pb chronology, SW Japan. Abstracts of the 123rd Annual Meeting of the Geological Society of Japan: 61.*

Hayashi, K., S. Fujita, K. Koarai and M. Matsukawa. 2017. Stratigraphy and paleoenvironment of the Cretaceous Sasayama Group in the Sasayama area, Hyogo Prefecture, western Japan. Journal of the Geological Society of Japan 123: 747–764.**

Hirasawa, S., K. Kashiwagi and M. Fujita. 2010. Marine strata and dinosaur footprints of the Upper Jurassic to Lower

Cretaceous Tetori Group, Toyama Prefecture. Journal of the Geological Society of Japan 116, Supplement: 103–121.*

Horn, I., and F. V. Blanckenburg. 2007. Investigation on elemental and isotopic fractionation during 196 nm femtosecond laser ablation multiple collector inductively coupled plasma mass spectrometry. Spectrochimica Acta B62: 410–422.

Hurford, A. J. 1986. Cooling and uplift patterns in the Lepontine Alps South Central Switzerland and an age of vertical movement on the Insubric fault line. Contributions to Mineralogy and Petrology 92 : 413–427.

International Commission on Stratigraphy. 2018. International Chronostratigraphic Chart, v 2018/08. http://www.stratigraphy.org/ICSchart/ChronostratChart2018-08.pdf.

Kawagoe, Y., S. Sano, Y. Orihashi, H. Obara, Y. Kouchi and S. Otoh. 2012. New detrital zircon age data from the Tetori Group in the Mana and Itoshiro areas of Fukui Prefecture, Central Japan. Memoir of the Fukui Prefectural Dinosaur Museum 11: 1–18.

Kawai, M. 1956. On the Late Mesozoic movement in the western part of Hida Plateau, part 1 (Geological study in the southern mountain-land of Arashimadake, Fukui Prefecture). Journal of the Geological Society of Japan 62: 559–573.**

Kawai, M. 1959. On the Late Mesozoic crustal movement in the western part of Hida Plateau, Central Honshu, Japan Part 2 (Geological study in the Echizen-Mino mountainland, Fukui and Gifu Prefectures). Journal of the Geological Society of Japan 65: 760–765.**

Kawai, M., and T. Nozawa. 1958. Geological Map of the Higashimozumi District. With Geological Sheet Map at 1:50,000. Geological Survey of Japan, 86 pp.**

Kouchi, Y., H. Obara, T. Fujimoto, Y. Orihashi, Y. Haruta and K. Yamamoto. 2015. Zircon U-Pb dating by 213 nm Nd YAG laser ablation inductively coupled plasma mass spectrometry. Optimization of the analytical condition to use NIST SRM 610 for Pb/U fractionation correction. Chikyukagaku (Geochemistry) 49: 19–35.**

Kozai, T., K. Ishida, S.-O. Park and K.-H. Chang. 2002. Early Cretaceous non-marine bivalves from Korea and Japan. Abstracts with Programs of the 2002 Annual Meeting of the Palaeontological Society of Japan: 16–17.

Kusuhashi, N., Y. Tsutsumi, H. Saegusa, K. Horie, T. Ikeda, K. Yokoyama and K. Shiraishi. 2013. A new Early Cretaceous eutherian mammal from the Sasayama Group, Hyogo, Japan. Proceedings of the Royal Society of London B: Biological Sciences 280: 20130142, doi: 10.1098/rspb.2013.0142.

Ludwig, K. R. 2012. Isoplot 3.75: Geochronological Toolkit for Microsoft Excel. Berkeley Geochronology Center Special Publication 5: 77 pp.

Maeda, S. 1957. The Tetori Group in the Oyama area, Itoshiro Village, Fukui Prefecture. The Journal of the Geological Society of Japan 63: 664–668.**

Maeda, S. 1961. On the geological history of the Mesozoic Tetori Group in Japan. Journal of the College of Arts and Science , Chiba University 3: 369–426.**

Maeda, S., and K. Takenami. 1957. Stratigraphy and geological structure of the Tetori Group in the southern district of Toyama Prefecture. The Journal of the Geological Society of Japan 63: 273–288.**

Matsui, K., Y. Kimura, M. Nagata, H. Inose, K. Ikeda, B. Beatty, H. Obayashi, T. Hirata, S. Otoh, T. Shinmura, S. Agematsu and K. Sashida. 2018. A long-forgotten "dinosaur" bone from a museum cabinet, uncovered to be a Japan's iconic extinct mammal. Royal Society Open Science 5: 172441, doi: 10.1098/rsos.172441.

Matsukawa, M., M. Fukui, Y. Ogawa, T. Tago, K. Koarai, H. Ohira and K. Hayashi. 2014a. Stratigraphy of the Tetori Group and the Jinzu Group (new name) in Gifu and Toyama prefectures, central Japan. Journal of the Geological Society of Japan 120: 147–164; 218–219.**

Matsukawa, M., M. Fukui, Y. Ogawa, T. Tago, K. Koarai and K. Hayashi. 2014b. Sedimentary environments and basin development of the Jinzu Group in the border area between Toyama and Gifu prefectures, central Japan. Journal of the Geological Society of Japan 120: 201–217.**

Matsukawa, M., T. Hamuro, T. Mizukami and S. Fujii. 1997. First trackway evidence of gregarious dinosaurs from the Lower Cretaceous Tetori Group of eastern Toyama Prefecture, central Japan. Cretaceous Research 18: 603–619.

Miyazaki, K., T. Ikeda, H. Matsuura, T. Danhara, H. Iwano and T. Hirata. 2018. Ascent of migmatites of a high-temperature metamorphic complex due to buoyancy beneath a volcanic arc: a mid-Cretaceous example from the eastern margin of Eurasia. International Geology Review (doi:10.1080/00206814.2018.1443403).

Sakai, Y., T. Ito, Y. Ibaraki, K. Yoshino, N. Ishida, T. Umetsu, K. Nakada, A. Matsumoto, T. Hinohara, K. Matsumoto and A. Matsuoka. 2012. Lithology and Stratigraphy of the Mizukamidani Formation of the Tetori Group in the right bank of the Sakaigawa River in the Itoigawa area, Niigata Prefecture, central Japan. Bulletin of the Itoigawa City Museums 3: 1–11.**

Sakai, Y., S. Sekido and A. Matsuoka. 2018. Stratigraphy of the Lower Cretaceous Tetori Group and stratigraphic implication of plant assemblages in the border area between Ishikawa and Fukui Prefectures, central Japan. Journal of the Geological Society of Japan 124: 171–189.**

Sakai, Y., T. Sonoda, Y. Tsutsumi, N. Kusuhashi, K. Horie and A. Matsuoka. 2015. Zircon U-Pb age of a tuff from the Akaiwa Subgroup, Tetori Group in the Shiramine area, Ishikawa Prefecture, Japan. Abstracts with Programs of the 2015 Annual Meeting of the Palaeontological Society of Japan: 49.*

Sano, S. 2015. New view of the stratigraphy of the Tetori Group in Central Japan. Memoir of the Fukui Prefectural Dinosaur Museum 14: 25–61.

Sato, T., and G. E. G. Westermann. 1991. Japan and South East Asia; pp. 81–108 *in* G. E. G. Westermann and A. C. Riccardi (eds.), Jurassic Taxa Ranges and Correlation Charts for the Circum Pacific 4, Newsletters on Stratigraphy 24. Schweizerbart Science Publishers, Stuttgart.

Shigeno, J. 2003. Sedimentary environment of the Jurassic–Cretaceous Tetori Group of Nagato River area, southern Toyama Prefecture. Journal of Science of the Hiroshima

University, Series C, 11: 133–154.

Stacey, J. T., and J. D. Kramers. 1975. Approximation of terrestrial lead isotope evolution by a two-stage model. Earth and Planetary Science Letters 26: 207–221.

Takeuchi, M., R. Furukawa. M. H. Nagamori and T. Oikawa. 2017. Geological Map of the Tomari District with Geological Sheet Map at 1:50,000. Geological Survey of Japan, AIST, 121 pp.**

Takeuchi, M., M. Ohkawa, K. Kawahara, S. Tomita, H. Yokota, T. Tokiwa and R. Furukawa. 2015. Redefinition of the Cretaceous terrigenous strata in the northeastern Toyama Prefecture based on U-Pb ages of zircon. Journal of the Geological Society of Japan 121: 1–17.**

Tanase, A., N. Yamada and K. Wakita. 1994. Hayashidani Andesite: 100 Ma calc-alkaline andesite in the uppermost reaches of Kuzuryu River, central Japan. Journal of the Geological Society of Japan 100: 635–638.*

Toyama Dinosaur Research Group. 2002. Report of the Dinosaur Excavation Project in 2000 & 2001, Toyama Prefecture, Japan. Toyama Dinosaur Research Group, 60 p.**

Wakita, K., S. Harayama, K. Kano, K. Mimura and T. Sakamoto. 1992. Geological Map of Japan 1: 200,000, Gifu. Geological Survey of Japan.*

Wiedenbeck, M., P. Allé, F. Corfu, W. L. Griffin, M. Meier, F. Oberli, A. von Quadt, J. C. Roddick and W. Spiegel. 1995. Three natural zircon standards for U-Th-Pb, Lu-Hf, trace element and REE analyses. Geostandards Newsletter 19: 1–23.

Yamada, K. 1988. Tetori Group; pp. 26–37 *in* N. Yamashita, Y. Kaseno and J. Itoigawa (eds.), Regional Geology of Japan Part 5 Chubu II. Kyoritsu Shuppan Co., Tokyo.**

Yamada, T. 2017. Study history of definitions on the Late Mesozoic Tetori Group in Central Japan and some proposals for future revision of the definition. Memoir of the Fukui Prefectural Dinosaur Museum 16: 55–70.**

* : in Japanese
** : in Japanese with English abstract

＜ 地名・地層名 ＞

Akaiwa Formation …… 赤岩層
Akaiwa Subgroup …… 赤岩亜層群
Asahi area …… 朝日地域
Asuwa Group …… 足羽層群
Atotsugawa Formation …… 跡津川層
Furukawa-Kamitakara area …… 古川・上宝地域
Gifu Prefecture …… 岐阜県
Gujo City …… 郡上市
Hakusan Region …… 白山区
Hayashidani Andesite …… 林谷安山岩
Hida Belt …… 飛騨帯
Hida City …… 飛騨市
Hida Gaien Belt …… 飛騨外縁帯
Hida Granite …… 飛騨花崗岩類
Higashisakamori Formation 東坂森層
Hiroshima Prefecture …… 広島県
Hyogo Prefecture …… 兵庫県
Inner Zone …… 内帯
Inotani Formation …… 猪谷層
Inotani Alternation Member …… 猪谷互層部層
Ioridani …… 庵谷
Ioridanitoge Conglomerate Member …… 庵谷峠礫岩部層
Ishikawa Prefecture …… 石川県
Itoshiro area …… 石徹白地域
Itoshirogawa River …… 石徹白川
Itoshiro-Oyama area … 石徹白・大山地域
Itoshiro Subgroup …… 石徹白亜層群
Iwaidani …… 岩井谷
Jinzu Group …… 神通層群
Jinzu Region …… 神通区
Jinzugawa River …… 神通川
Fukui Prefecture …… 福井県
Kanmon Group …… 関門層群
Katsuyama City …… 勝山市
Kisa Andesite …… 吉舎安山岩
Kitadani Formation …… 北谷層
Koyadanigawa River …… 小屋谷川
Kurokawa River …… 黒川
Kuzuryu Group …… 九頭竜層群
Kuzuryu Subgroup …… 九頭竜亜層群
Kuzuryugawa area …… 九頭竜川地域
Kuzuryugawa River …… 九頭竜川
Minamimatadani …… 南俣谷
Minamimatadani Conglomerate Member …… 南俣谷礫岩部層
Mizuhoradani …… 水洞谷
Mizukamidani Formation … 水上谷層
Monobegawa Group …… 物部川層群
Mt. Hakusan …… 白山
Nakanomatanokkoshi Sandstone Member …… 中俣乗越砂岩部層
Nagatogawa area …… 長棟川地域
Nagatogawa Formation …… 長棟川層
Niigata Prefecture …… 新潟県
Nobudani …… 延谷
Nobu-dani (Conglomerate) Formation …… 延谷礫岩層
Omodani Rhyolite …… 面谷流紋岩
Oshimizu …… 大清水
Oyama area …… 大山地域
Oyama Formation …… 大山層
Oyashirazu Formation …… 親不知層
Ryoseki Formation …… 領石層
Sasayama Group …… 篠山層群
Sawada Formation …… 沢田層
Shokawa area …… 荘川地域
Shimonomoto …… 下之本
Shimonoseki Subgroup … 下関亜層群
Shimozaisho Group …… 下在所層群
Southwest Japan …… 西南日本
Takigadani …… 滝ヶ谷
Takinami area …… 滝波地域
Tedorigawa area …… 手取川地域
Tedorigawa River …… 手取川
Tetori Group …… 手取層群
Toyama City …… 富山市
Toyama Prefecture …… 富山県
Utsubodani …… 打保谷
Utsubodanigawa River …… 打保谷川
Wasabu …… 和佐府
Wasabu Alternation Member …… 和佐府互層部層
Yamaguchi Prefecture …… 山口県
Yamanomura area …… 山之村地域